Growth of the lava dome and extrusion rates at Soufrière Hills Volcano, Montserrat, West Indies: 2005–2008

G. A. Ryan,[1,2,3] S. C. Loughlin,[1,4] M. R. James,[5] L. D. Jones,[1,2] E. S. Calder,[6] T. Christopher,[1,2] M. H. Strutt,[1,2] and G. Wadge[7]

Received 18 November 2009; revised 24 January 2010; accepted 4 February 2010; published XX Month 2010.

[1] The third episode of lava dome growth at Soufrière Hills Volcano began 1 August 2005 and ended 20 April 2007. Volumes of the dome and talus produced were measured using a photo-based method with a calibrated camera for increased accuracy. The total dense rock equivalent (DRE) volume of extruded andesite magma (306 ± 51 Mm^3) was similar within error to that produced in the earlier episodes but the average extrusion rate was 5.6 ± 0.9 m^3s^{-1} (DRE), higher than the previous episodes. Extrusion rates varied in a pulsatory manner from <0.5 m^3s^{-1} to ~20 m^3s^{-1}. On 18 May 2006, the lava dome had reached a volume of 85 Mm^3 DRE and it was removed in its entirety during a massive dome collapse on 20 May 2006. Extrusion began again almost immediately and built a dome of 170 Mm^3 DRE with a summit height 1047 m above sea level by 4 April 2007. There were few moderate-sized dome collapses (1–10 Mm^3) during this extrusive episode in contrast to the first episode of dome growth in 1995–8 when they were numerous. The first and third episodes of dome growth showed a similar pattern of low (<0.5 m^3s^{-1}) but increasing magma flux during the early stages, with steady high flux after extrusion of ~25 Mm^3. **Citation:** Ryan, G. A., S. C. Loughlin, M. R. James, L. D. Jones, E. S. Calder, T. Christopher, M. H. Strutt, and G. Wadge (2010), Growth of the lava dome and extrusion rates at Soufrière Hills Volcano, Montserrat, West Indies: 2005–2008, *Geophys. Res. Lett.*, *37*, LXXXXX, doi:10.1029/2009GL041477.

1. Introduction

[2] The ongoing eruption of the Soufrière Hills Volcano (SHV) on Montserrat began on 18 July 1995 [*Young et al.*, 1998] and has involved three major episodes of lava dome growth: the first from 15 November 1995 to 10 March 1998 [*Norton et al.*, 2002; *Sparks et al.*, 1998]; the second from November 1999 until 28 July 2003 [*Herd et al.*, 2005]; and the third from 1 August 2005 until 20 April 2007. A fourth episode of dome growth began in August 2008. Monitoring the extrusion rate of the lava and volumetric and morphological changes of the growing lava dome at SHV are critical to the effective assessment of volcanic hazards, particularly pyroclastic flows, surges and explosions [*Calder et al.*, 2002; *Sparks et al.*, 1998; *Watts et al.*, 2002].

[3] This paper focuses on the third episode of lava dome growth. It was notable for the highest recorded lava extrusion rates to date, the fewest significant dome collapses (and associated pyroclastic flows) and a lack of hybrid earthquake seismicity [*Luckett et al.*, 2008]. We describe the methods used by Montserrat Volcano Observatory (MVO) to assess dome volume and extrusion rate, discuss pyroclastic flow and tephra volumes, and show how morphological and dynamic variations in lava dome growth are related to extrusion rates and volume.

2. Methods

[4] Four methods were used to assess lava dome volume during the third episode of dome growth: 1) a terrestrial photo-method; 2) ground-based LiDAR [*Jones*, 2006]; 3) a prototype ground-based radar (AVTIS: All-weather Volcano Topographic Imaging Sensor [*Robertson and Macfarlane*, 2006; *Wadge et al.*, 2005, 2008], and 4) an empirical method that uses photographs of dome profiles and assumes proportionality between the pixel area of an image of the dome and the volume of the dome (not considered further here). The first three techniques measure the coordinates of points on the growing lava dome and enable the generation of a 3D surface representing the dome and talus. Only the terrestrial photo-method was used regularly. Spatial coordinates of points on the dome were calculated from oblique-view digital image pairs taken from known locations on the same day with a camera that had been pre-calibrated using the MATLAB™ camera calibration toolbox available at http://www.vision.caltech.edu/bouguetj/calib_doc/index.html. Volcanic hazards prevented the deployment of control point targets, so camera orientations were calculated using features in the images that had been coordinated by theodolite measurements. Data were processed using in-house software based on the MATLAB camera calibration toolbox.

[5] A Canon EOS Digital Rebel XT with a Canon EFS 18–55 mm zoom lens set at the 18 mm position was used to take all photographs. A set of 25 photographs of a flat chess board in different orientations were the input data for the camera calibration. The details of camera calibration are described by *Zhang* [2005]. The use of the intrinsic camera model generated by camera calibration increased the accuracy of the photo-method.

[1]Montserrat Volcano Observatory, Flemmings, Montserrat.
[2]British Geological Survey, Keyworth, UK.
[3]Now at Institute of Earth Science and Engineering, University of Auckland, Auckland, New Zealand.
[4]British Geological Survey, Edinburgh, UK.
[5]Lancaster Environment Centre, Lancaster University, Lancaster, UK.
[6]Department of Geology, State University of New York at Buffalo, Buffalo, New York, USA.
[7]Environmental Systems Science Centre, University of Reading, Reading, UK.

0094-8276/10/2009GL041477$05.00

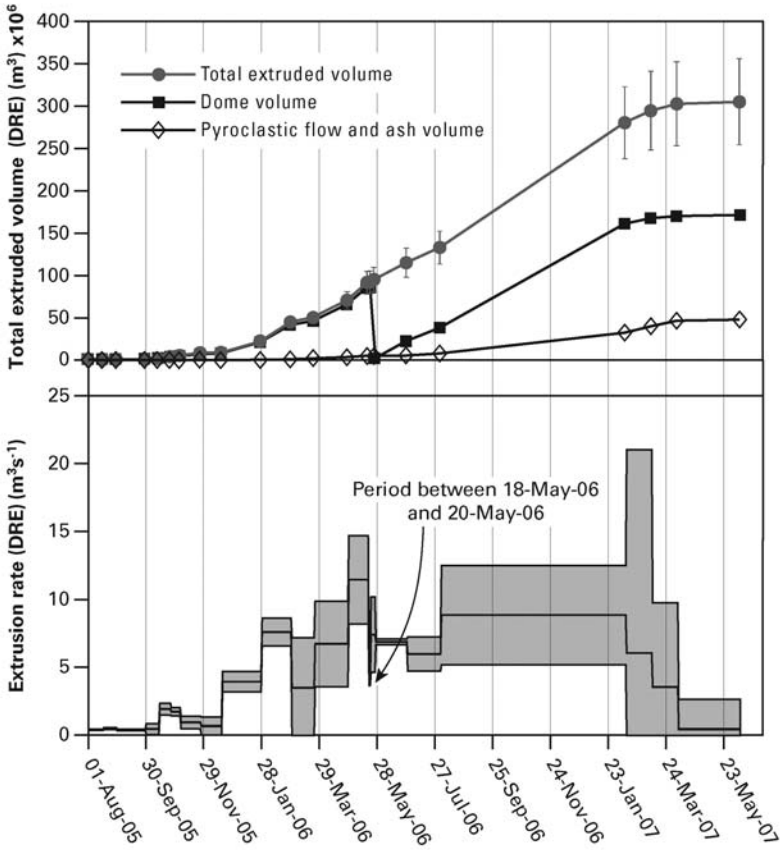

Figure 1. Total extruded magma volume (DRE) during the third episode of dome growth. Total volume is the sum of measured lava dome volume and volume of pyroclastic flow and associated ash deposits. Error bars reflect a 15% error dominated by systematic errors. The horizontal central lines in magma extrusion rates (DRE) are average rates over the periods between dome volume measurements. The grey shading indicates errors associated with extrusion rates (see text). The 20 May 2006 dome collapse is represented by a sharp decrease in dome volume around that date. The extrusion rate for the period between 18 May 2006 and 20 May 2006 was estimated at the average rate for the dome growth episode up to that time (3.7 m^3s^{-1}). There are no error bars associated with this estimate on the graph and it has the appearance of a vertical dark line in the extrusion rate graph.

[6] The coordinates produced by the photo or LiDAR methods were interpolated using Kriging algorithms in ArcGIS9 to create a 3D representation of the dome. The resulting digital elevation model was compared visually to photographs of the dome and minor changes were made to the model to obtain a good match (Figure 1). Each successive model could then be subtracted from the previous one to yield a volume change.

[7] Each of the volume increments includes dense and vesicular lava, numerous shear and fracture zones and talus. Following the methodology of *Sparks et al.* [1998], the MVO has over the years calculated DRE by assuming an average 13% vesicularity and 3% void space in talus, giving a multiplicative correction factor of 0.844 to convert from measured dome volume to dense rock equivalent (DRE). The bulk vesicularity and pore space in the dome (including talus) vary through time and cannot be measured, there is therefore considerable uncertainty. We use these values so that volumes and extrusion rates can be compared to previously published data. *Wadge et al.* [2010] used slightly different bulk densities and pore space assumptions in their estimates for the whole eruption.

[8] The volume of pyroclastic flow deposits was estimated from field measurements where possible or calculated from an empirical relationship (with upper and lower bounds) between runout distance and volume established by *Calder et al.* [1999]. Conversion to DRE volumes was made assuming that dense andesitic lava has a density of 2600 kg/m^3 and the bulk density of pyroclastic flow deposits is 2000 kg/m^3 (i.e., using a conversion factor of 0.77 as used by *Sparks et al.* [1998]). Ash fall deposits were assumed to comprise an additional 15% of the pyroclastic flow deposit DRE volumes [*Sparks et al.*, 1998]; although detailed analysis [*Bonadonna et al.*, 2002] suggests that this is a maximum estimate.

3. Data Limitations

[9] The photo-method described is similar to the photographic method used by *Sparks et al.* [1998] for the first episode of lava dome growth but the use of a calibrated camera lens and the more precise determination of measurement points from digital images rather than from printed film increases the accuracy of the three dimensional point measurements. Nevertheless, photographic surveys of the

t1.1 **Table 1.** Measured Dome Volumes Using the Photo-Method[a]

t1.2 Dates	Measured Dome Volume (Mm^3) (Last Date)	Cumulative Dome Volume DRE (Mm^3)	Average Cumulative PF+ash DRE (Mm^3)	Average Cumulative PF+ash Error (Mm^3)	Cumulative Magma Volume DRE (Mm^3)	Average Extrusion Rate DRE (m^3/s)	Extrusion Rate Error (m^3/s)
t1.3 1–16 Aug 05	0.6	0.5	0	0	0.5 (0.37)	0.41	0.03
t1.4 16–30 Aug 05	1.3	1.1	0	0	1.1 (0.78)	0.48	0.06
t1.5 30 Aug–29 Sep 05	2.5	2.1	0	0	2.1 (1.09)	0.38	0.04
t1.6 29 Sep–13 Oct 05	3.0	2.5	0.15	0.09	2.7 (2.13)	0.46	0.39
t1.7 13–25 Oct 05	5.3	4.5	0.15	0.09	4.7 (4.61)	1.9	0.42
t1.8 25 Oct–4 Nov 05	7.1	6.0	0.15	0.09	6.1 (6.32)	1.7	0.29
t1.9 4–25 Nov 05	8.8	7.4	0.43	0.2	7.9 (8.16)	0.94	0.44
t1.10 25 Nov–17 Dec 05	9.9	8.4	0.79	0.5	9.1 (9.54)	0.68	0.65
t1.11 17 Dec–27 Jan 06	25.8	21.8	1.4	1.0	23.1 (22.25)	3.9	0.75
t1.12 27 Jan–27 Feb 06	49.6	41.9	1.7	1.2	43.5 (41.77)	7.6	1.0
t1.13 27 Feb–23 Mar 06	55.3	46.7	4.1	3.1	50.8 (46.76)	3.5	3.7
t1.14 23 Mar–27 Apr 06	78.4	66.2	5.0	3.7	71.1 (67.81)	6.7	3.2
t1.15 27 Apr–18 May 06	101	85.2	6.7	4.8	91.9 (87.96)	11.5	3.3
t1.16 18–20 May 06	N/A	85.9[b]	6.7	4.8	92.6*	3.7*	N/A
t1.17 20–25 May 06	3.8	89.1	6.7	4.8	95.8 (91.77)	7.4	2.8
t1.18 25 May–27 Jun 06	27.0	109	6.8	4.8	115 (110.04)	6.9	0.21
t1.19 27 Jun–1 Aug 06	46.0	125	8.8	5.8	134 (127.6)	6.0	1.3
t1.20 1 Aug–9 Feb 07	191	247	33.5	20.1	281 (262.58)	8.9	3.7
t1.21 9 Feb–8 Mar 07	199	254	40.9	26.5	295 (274.41)	6.1	15.0
t1.22 8 Mar–4 Apr 07	201	255	47.5	31.7	303 (283.59)	3.6	6.2
t1.23 4 Apr–08 Jun 07	203	257	48.8	32.7	306 (284.75)	0.4	2.2

t1.24 [a]LiDAR measurements in bold, calculated (DRE) volumes and average extrusion rates through episode three. Values in parentheses in the cumulative
t1.25 volume column are the equivalent values from the accounting method of *Wadge et al.* [2010] which uses a different bulk density for the talus.
t1.26 [b]Extruded volume for 20 May 06 is determined using the average extrusion rate up to 18 May 06 (3.7 m^3s^{-1}).

lava dome could only be carried out from two locations on the south and southeast sides of the crater so detailed surveys of the western and northwestern sides of the dome were not possible. Systematic error arises from the interpolation of the western side of the dome and uncertainty due to the assumptions of bulk density of the deposits. Systematic errors on the final interpolated volumes are estimated to be about 15% [*Sparks et al.*, 1998]. Random error is controlled by the errors in the dome point coordinate estimates which are of the order of 1 m. Assuming the dome is roughly hemispherical, the random error in the measured dome volume (σ_V) can be estimated by:

$$\sigma_V = \frac{2\pi\sigma_X}{\sqrt{n}}\left(3V/2\pi\right)^{2/3} \quad (1)$$

where σ_X is the coordinate error (~1 m), n is the number of point measurements on the dome surface and V is the estimated volume of the dome.

[10] The error on the change in extruded magma volume between measurements ($\sigma_{\Delta V}$) is given by the following equation:

$$\sigma_{\Delta V} = \left[(\sigma_{V_2})^2 + (\sigma_{V_1})^2 + (\sigma_{V_{PF1}})^2 + (\sigma_{V_{PF2}})^2\right] \quad (2)$$

where σ_{V_2} and σ_{V_1} are the random errors on the dome volume estimates and $\sigma_{V_{PF1}}$ and $\sigma_{V_{PF2}}$ are the errors on the pyroclastic flow volume estimates. Errors in extrusion rate will be dominated by random (rather than systematic) errors in dome volume estimates and errors in pyroclastic flow volume estimates.

[11] The error on the estimated extrusion rate is given by the following equation:

$$\sigma_Q = Q\left[\left(\frac{\sigma_{\Delta V}}{\Delta V}\right)^2 + \left(\frac{\sigma_{\Delta t}}{\Delta t}\right)^2\right]^{1/2} \quad (3)$$

Surveys of the dome were achieved on average once every two weeks due to infrequent helicopter access and low cloud. As a result, short-period variations in extrusion rate were not possible using either the LiDAR or photo-method. When operational, a permanently mounted mm-wave radar AVTIS 2, could potentially produce daily variations in extrusion rate [*Wadge et al.*, 2008].

4. Volumes and Extrusion Rates

[12] The total cumulative lava extrusion during the third episode of lava dome growth is calculated as the sum of the lava dome (including talus), pyroclastic flow and ash fall deposit volumes (all converted to DRE) at the times of the 21 surveys (Table 1 and Figure 2). The total volume of magma produced during the third episode of lava dome growth was 306 ± 51 Mm^3 based on the following: a total measured volume of extruded lava using the photo and LiDAR methods of 256 Mm^3 ± 38 Mm^3; a total volume of pyroclastic flow deposits (not including those associated with the 20 May 2006 event) using *Calder et al.*'s [1999] method of 14–67 Mm^3 (av. 40 Mm^3) and a tephra fall volume of 2–10 Mm^3 (av. 6 Mm^3).

[13] From the 21 surveys the DRE average extrusion rates have been calculated for 20 intervals (Table 1). The third episode of lava extrusion began with low average extrusion rates (up to 0.5 m^3s^{-1}), increasing to ~2 m^3s^{-1} on 13 October, an increase to ~4 m^3s^{-1} in mid-December and a significant increase on 10 February 2006 when the dome had reached a volume of about 25 Mm^3 DRE (Figures 2 and 3). Interestingly, a similar pattern of increasing flux occurred during growth of the first dome [*Sparks et al.*, 1998]. The average extrusion rate for the third phase of dome growth was 5.6 ± 0.9 m^3s^{-1} DRE, higher than both of the previous dome growth episodes (first episode 4.3 m^3s^{-1} DRE; second episode ~2 m^3s^{-1} [*Herd et al.*, 2005]). There were pulses of more

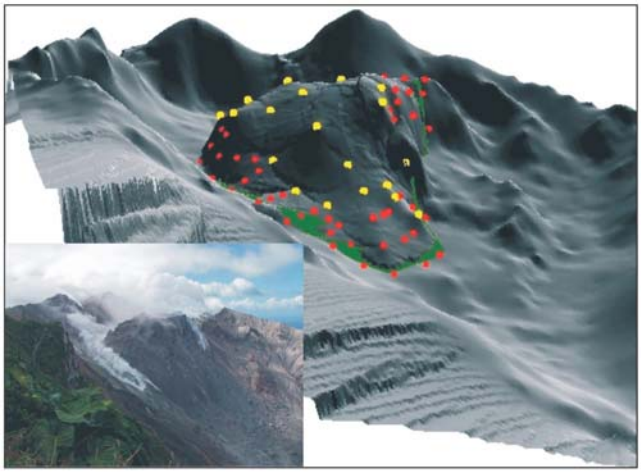

Figure 2. Three-dimensional dome model for 25 November 2005. The yellow dots represent point coordinates generated using the photo-method, the red points are points along a linear interpolation from the measured points to the base of the dome model. The dome model rests inside a DEM of the 2003–5 crater [*Herd et al.*, 2005].

vigorous dome growth, such as in February and December 2006, correlating with increased rockfall activity (>150 seismically-recorded events per day) as in dome growth episode one. There were periods of several days with no visible dome growth (<0.5 m^3s^{-1}) and periods of several weeks at 10 m^3s^{-1} and above. Survey intervals typically varied from 2 to 4 weeks, so shorter period extrusion rate variations are not represented in Table 1. For example, visual observations found no dome growth from 29 January to 9 February 2006 or from 24 to 25 February so the average rate for the period 27 January to 27 February (Table 1) was >12 m^3s^{-1} and the peak rate for 10–12 February may have exceeded 20 m^3s^{-1}.

[14] A LiDAR survey of the lava dome was carried out on 18 May 2006, and then the entire dome and parts of the crater floor and rim collapsed on 20 May 2006. Extrusion began again at a moderate rate on the same day, probably because there was only minimal involvement of the conduit during the collapse [*Luckett et al.*, 2008]. This was the only significant lava dome collapse during the whole dome growth period. Pyroclastic flows with measured volume >1 Mm^3 occurred on only two other occasions: 30 June 2006 (~2 Mm^3) and 8 January 2007 (a single flow of 5 Mm^3 and later discrete but persistent flows with a combined volume <5 Mm^3). Smaller pyroclastic flows with volumes <1 Mm^3 occurred on 149 separate days.

5. Discussion

[15] Episode three was characterised by a tendency for the lava dome to grow very large with relatively few small to moderate block-and-ash flows, and yet shear lobes and other morphological features developed in the same way as the first episode of lava dome growth and with the same relationship to extrusion rates [*Watts et al.*, 2002]. Extensive talus slopes developed but derived mainly from degassed dome rock in rockfalls [*Wadge et al.*, 2009]. During periods of high magma supply rate the extrusion of lower viscosity 'pancake' lobes [*Watts et al.*, 2002] tended to restore the sometimes irregularly-shaped edifice to a more symmetrical, flat-topped 'dome'. This process may, at times, have contributed to the dome's overall stability.

[16] Both the first and third episodes were preceded by about 4 months of phreatic activity showing similar surface responses to events at depth. At the beginning of episode three, average extrusion rates remained low (<0.5 m^3s^{-1}) for 74 days and produced 2.5 Mm^3 DRE of magma, remarkably similar to the first dome growth episode in which slow growth (<0.6 m^3s^{-1} DRE) lasted 77 days [*Sparks et al.*, 1998] and produced about 2.2 Mm^3 magma (Figure 3). This behaviour during the first episode was interpreted by *Sparks et al.* [1998] as being caused by degassed, highly viscous magma that had been infilling the conduit for several months before extrusion began, inhibiting the flow rate. Assuming a cylindrical conduit of diameter 30m [*Devine et al.*, 1998; *Melnik and Sparks*, 1999] these magma volumes would fill the conduit to a depth of <3.5km. Alternatively, *Costa et al.* [2007] and *Hautmann et al.* [2009] suggest a model in which a cylindrical conduit at the surface becomes a dyke at depth which would decrease this estimate. Episode three was shorter than episode one (627 and 846 days respectively) and average and peak extrusion rates were higher, implying a high magma driving pressure. High extrusion rates during episode one were linked to pulses of volatile-rich magma [*Sparks et al.*, 1998; *Voight et al.*, 1999]. The high numbers of long-period rockfall and rockfall seismic events in April–May 2006 implied high gas pressures consistent with high sulphur dioxide emissions during the 20 May 2006 dome collapse [*Loughlin et al.*, 2006]. During a peak in activity on 8 January 2007, some erupted pumice contained >6 wt% H_2O, the highest recorded in the whole eruption [*Humphreys et al.*, 2009] implying that the link between volatile content and extrusion

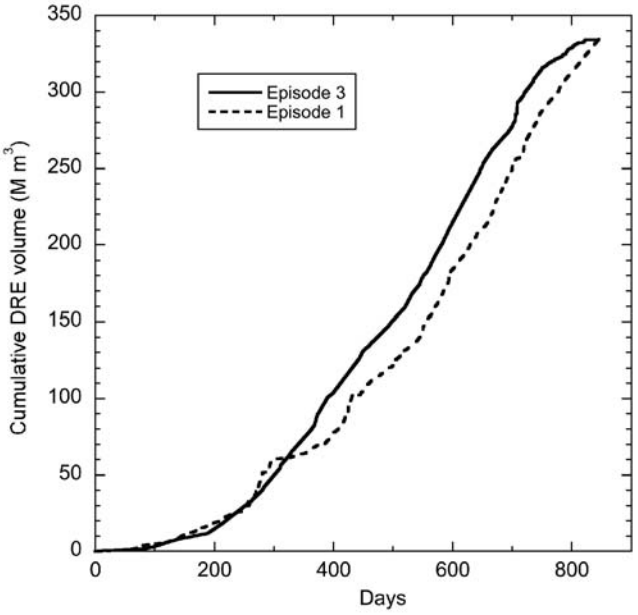

Figure 3. Cumulative dome volumes for dome growth episode 1 with dome growth episode 3 cumulative volumes normalised for duration superimposed. The major dome collapse and explosion in 17 September 1996 [*Robertson et al.*, 1998] caused the subsequent temporary decrease in magma flux.

rate continued after the 20 May collapse. The similarities between dome growth episodes one and three suggest that despite a possible small overall increase in average volatile content (causing higher overall average extrusion rates), possible increased fracturing of the conduit walls [*Luckett et al.*, 2008], and tendency in 2005–07 to major collapses, the fundamental dynamics of this eruption did not change significantly in nearly 12 years.

[17] **Acknowledgments.** The authors gratefully acknowledge the assistance of MVO staff in the collection of the data presented here. The authors publish with the permission of the Executive Director of the British Geological Survey. GW acknowledges the support of NERC grant NE/E001734/1. MRJ was funded by NE/E001734/1 and the Royal Society.

References

Bonadonna, C., et al. (2002), Tephra fallout in the eruption of Soufrière Hills Volcano, Montserrat, in *The Eruption of Soufrière Hills Volcano, Montserrat, From 1995 to 1999*, edited by T. H. Druitt and B. P. Kokelaar, *Geol. Soc. London Mem.*, *21*, 483–516.

Calder, E. S., P. D. Cole, W. B. Dade, T. H. Druitt, R. P. Hoblitt, H. E. Huppert, L. Ritchie, R. S. J. Sparks, and S. R. Young (1999), Mobility of pyroclastic flows and surges at the Soufrière Hills Volcano, Montserrat, *Geophys. Res. Lett.*, *26*(5), 537–540, doi:10.1029/1999GL900051.

Calder, E. S., R. Luckett, R. S. J. Sparks, and B. Voight (2002), Mechanisms of lava dome instability and generation of rockfalls and pyroclastic flows at Soufrière Hills Volcano, Montserrat, in *The Eruption of Soufrière Hills Volcano, Montserrat, From 1995 to 1999*, edited by T. H. Druitt and B. P. Kokelaar, *Geol. Soc. London Mem.*, *21*, 173–190.

Costa, A., O. Melnik, R. S. J. Sparks, and B. Voight (2007), Control of magma flow in dykes on cyclic lava dome extrusion, *Geophys. Res. Lett.*, *34*, L02303, doi:10.1029/2006GL027466.

Devine, J. D., M. J. Rutherford, and J. E. Gardner (1998), Petrologic determination of ascent rates for the 1995–1997 Soufrière Hills Volcano andesitic magma, *Geophys. Res. Lett.*, *25*(19), 3673–3676, doi:10.1029/98GL00912.

Hautmann, S., J. Gottsmann, R. S. J. Sparks, A. Costa, O. Melnik, and B. Voight (2009), Modelling ground deformation caused by oscillating overpressure in a dyke conduit at Soufrière Hills Volcano, *Montserrat, Tectonophysics*, *471*(1–2), 87–95, doi:10.1016/j.tecto.2008.10.021.

Herd, R. A., M. Edmonds, and V. A. Bass (2005), Catastrophic lava dome failure at Soufrière Hills Volcano, Montserrat, 12–13 July 2003, *J. Volcanol. Geotherm. Res.*, *148*(3–4), 234–252, doi:10.1016/j.jvolgeores.2005.05.003.

Humphreys, M. C. S., M. Edmonds, T. Christopher, and V. Hards (2009), Chlorine variations in the magma of Soufrière Hills Volcano, Montserrat: Insights from Cl in hornblende and melt inclusions, *Geochim. Cosmochim. Acta*, *73*(19), 5693–5708, doi:10.1016/j.gca.2009.06.014.

Jones, L. D. (2006), Monitoring landslides in hazardous terrain using terrestrial LiDAR: An example from Montserrat, *Q. J. Eng. Geol. Hydrol.*, *39*, 371–373, doi:10.1144/1470-9236/06-009.

Loughlin, S. C., et al. (2006), Report to the Scientific Advisory Committee Montserrat, August 2006 (06/07), open file report, Montserrat Volcano Obs., Flemmings, Montserrat.

Luckett, R., S. Loughlin, S. De Angelis, and G. Ryan (2008), Volcanic seismicity at Montserrat, a comparison between the 2005 dome growth episode and earlier dome growth, *J. Volcanol. Geotherm. Res.*, *177*(4), 894–902, doi:10.1016/j.jvolgeores.2008.07.006.

Melnik, O., and R. S. J. Sparks (1999), Nonlinear dynamics of lava dome extrusion, *Nature*, 402(6757), 37–41, doi:10.1038/46950.

Norton, G. E., et al. (2002), Pyroclastic flow and explosive activity of the lava dome at Soufrière Hills Volcano, Montserrat, during a period of no magma extrusion (March 1998 to November 1999), in *The Eruption of Soufrière Hills Volcano, Montserrat, From 1995 to 1999*, edited by T. H. Druitt and B. P. Kokelaar, *Geol. Soc. London Mem.*, *21*, 467–481.

Robertson, D. A., and D. G. Macfarlane (2006), A 94 GHz dual-mode imaging "radarometer" for remote sensing, *Proc. SPIE*, *6211*, 621102, doi:10.1117/12.669668.

Sparks, R. S. J., et al. (1998), Magma production and growth of the lava dome of the Soufrière Hills Volcano, Montserrat, West Indies: November 1995 to December 1997, *Geophys. Res. Lett.*, *25*(18), 3421–3424, doi:10.1029/98GL00639.

Voight, B., et al. (1999), Magma flow instability and cyclic activity at Soufrière Hills volcano, Montserrat, British West Indies, *Science*, *283*(5405), 1138–1142, doi:10.1126/science.283.5405.1138.

Wadge, G., D. G. Macfarlane, D. A. Robertson, A. J. Hale, H. Pinkerton, R. V. Burrell, G. E. Norton, and M. R. James (2005), AVTIS: A novel millimetre-wave ground based instrument for volcano remote sensing, *J. Volcanol. Geotherm. Res.*, *146*(4), 307–318, doi:10.1016/j.jvolgeores.2005.03.003.

Wadge, G., et al. (2008), Lava dome growth and mass wasting measured by a time series of ground-based radar and seismicity observations, *J. Geophys. Res.*, *113*, B08210, doi:10.1029/2007JB005466.

Wadge, G., G. Ryan, and E. S. Calder (2009), Clastic and core lava components of a silicic lava dome, *Geology*, *37*(6), 551–554, doi:10.1130/G25747A.1.

Wadge, G., R. Herd, G. Ryan, E. S. Calder, and J.-C. Komorowski (2010), Lava production at Soufrière Hills Volcano, Montserrat: 1995–2009, *Geophys. Res. Lett.*, *37*, L00E03, doi:10.1029/2009GL041466.

Watts, R. B., R. A. Herd, R. S. J. Sparks, and S. R. Young (2002), Growth patterns and emplacement of the andesite lava dome at Soufrière Hills Volcano, in *The Eruption of Soufrière Hills Volcano, Montserrat, From 1995 to 1999*, edited by T. H. Druitt and B. P. Kokelaar, *Geol. Soc. London Mem.*, *21*, 115–152.

Young, S. R., R. S. J. Sparks, W. P. Aspinall, L. L. Lynch, A. D. Miller, R. E. A. Robertson, and J. B. Shepherd (1998), Overview of the eruption of Soufrière Hills Volcano, Montserrat, 18 July 1995 to December 1997, *Geophys. Res. Lett.*, *25*(18), 3389–3392, doi:10.1029/98GL01405.

Zhang, Z. (2005), Camera calibration, in *Emerging Topics in Computer Vision*, edited by G. Medioni and S. B. Kang, pp. 4–43, Prentice Hall, Upper Saddle River, N. J.

E. S. Calder, Department of Geology, State University of New York at Buffalo, Buffalo, NY 14260, USA.

T. Christopher, L. D. Jones, and M. H. Strutt, Montserrat Volcano Observatory, Flemmings, Salem, Montserrat, West Indies.

M. R. James, Lancaster Environment Centre, Lancaster University, Lancaster LA1 4YQ, UK.

S. C. Loughlin, British Geological Survey, West Mains Road, Edinburgh EH9 3LA, UK.

G. A. Ryan, Institute of Earth Science and Engineering, University of Auckland, PB 92019, Auckland 1142, New Zealand. (g.ryan@auckland.ac.cz)

G. Wadge, Environmental Systems Science Centre, University of Reading, Reading RG6 6AL, UK.